Mechanical and Energy Engineering

Thermal Buckling Analysis of Laminated Composite plates with General Elastic Boundary Supports

Mohammed Basheer Hammed
MSc student
College of Engineering- University of Baghdad
Email:mohammed88alabas@gmail.com

Dr. Wedad Ibrahim Majid*
Assistant professor
College of Engineering-University of Baghdad
Email: wedad.ibrahim@coeg.uobaghdad.edu.iq

ABSTRACT

In this study, the modified Rayleigh-Ritz method and Fourier series are used to determine the thermal buckling behavior of laminated composite thin plates with a general elastic boundary condition applied to in-plane uniform temperature distribution depending upon classical laminated plate theory(CLPT). A generalized procedure solution is developed for the Rayleigh-Ritz method combined with the synthetic spring technique. The transverse displacement of the orthotropic rectangular plates is not a different term as a new shape expansion of trigonometric series. In this solution approach, the plate transverse deflection and rotation due to bending are developed into principle Fourier series with a sufficient smoothness auxiliary polynomial function, the variable of boundary condition can be easily done by only change the boundary spring stiffness of at the all boundaries of laminated composite plate without achieving any replacement to the solution. The accuracy of the current outcome is verified by comparing with the result obtained from other analytical methods in addition to the finite element method (FEM), so the excellent of this technique is proving during numerical examples.

Keywords: Composite laminated plate, thermal buckling, general boundary condition, Rayleigh-Ritz method.

الانبعاج الحراري لطبقة من الصفائح المركبة مع اسناد حافات مرنة وعامة

محمد بشير حميد

وداد ابراهيم ماجد

طالب ماجستير

استاذ مساعد

جامعة بغداد – كلية الهندسة – قسم الهندسة الميكيانيكية

جامعة بغداد – كلية الهندسة – قسم الهندسة الميكيانيكية

الخلاصة

في هذه الدراسة ، يتم استخدام طريقة Rayleigh–Ritz المعدلة وسلسلة Fourier لتحديد سلوك الانبعاج الحراري للصفائح الرفيعة المركبة مع اسناد مختلف وعام مرن لحافاتها المطبقة في توزيع درجة حرارة موحدة اعتمادًا على نظرية الألواح الرقائقي الكلاسيكية (CLPT). تم تطوير حل إجراء معمم لطريقة Rayleigh–Ritz مقترنة بتقنية النابض الاصطناعية ، الإزاحة المستعرضة للصفائح المستطيلة التقويمية لا تختلف عن المصطلح كتوسعات شكل جديدة لسلسلة مثلثية. في نهج الحل هذا ، يتم تطوير انحراف الدوران العرضي للوحة والدوران بسبب الانحناء إلى سلسلة Fourier ذات وظيفة متعددة الحدود بنعومة

كافية، ويمكن إجراء تباين حالة الحدود بسهولة فقط عن طريق تغيير صلابة النابض الحدودي في جميع حدود مركبة لوحة مغلفة دون تحقيق أي تغيير للحل. يتم التحقق من دقة النتائج الحالية من خلال المقارنة مع النتائج التي تم الحصول عليها من طريقة تحليلية أخرى بالإضافة إلى طريقة العناصر المحدودة (FEM)، لذلك فإن إثبات هذه التقنية ممتاز خلال الأمثلة العددية.

الكلمات الرئيسية: طبقات لصفائح مركبة، الانبعاج الحراري، حافات اسناد عامة، طريقة.Rayleigh–Ritz.

1. INTRODUCTION

The materials composite is widely employed in different enforcement, engineering specialties in mechanical and civil engineering, each type of composites are suitable for a particular temperature range and may behave elastically, but has variable mechanical properties and thermal expansion characteristics. Therefore, it is important to predict the thermal buckling response of temperature-sensitive multilayered composite plates. Lots have been researched about thermal analysis of buckling laminated composite thick plates and thin, but the research has been focused on some problems that include a few forms of boundary conditions because the rectangular plate has 55 forms of boundary condition, therefore, the solution procedure becomes very tedious when using mode shapes as the basis functions, that's why the former researchers had used at least opposite edges of one pair of simply supported and clamped, so with all boundary conditions one may have to apply convergent methods like the method of Rayleigh-Ritz. The choosing of suitable admissible functions is of high significance when applying the method of Rayleigh-Ritz due to precision of the results; many investigations had researched about thermal buckling of laminated plate by using classical laminated plate theory but no one study with general boundary condition by using spring technique. **(Hiroyuki Matsunaga, 2006)**. presented a two-dimensional global higher-order deformation theory for thermal buckling angle-ply laminated composite and sandwich plates, using the method of the power series expansion of continuous displacement components after the differential equations of higher order is solved, the effects of the 3D layerwise theory and the theory are refined of angle-ply laminated thermal buckling. **(Houdayfa OUNIS, et al., 2014)** studied the thermal buckling behavior of composite laminated plates under a uniform temperature distribution. A finite element of 32 degrees of freedom (DOF) and four nodes. The finite element is a collection of a high precision rectangular Hermitian element and linear isoparametric membrane element, based upon the classical plate theory. Parametrical research also leads to determining the influence of the composite material anisotropy on the critical temperature of buckling laminated plates. The investigation presented that: 1) orientation angles and the boundary conditions influenced the critical buckling temperature of laminated plates, and 2) the critical temperature of buckling reduces with the rising of ratio thermal expansion α_T/α_L and the modulus ratio E_L/E_T. **(A.R.Vosoughi and M.R. Nikoo, 2015)** presented the together fundamental maximizing the natural frequency and critical temperature of backing laminated composite plates within a modern incorporation of the Young bargaining model, the differential quadrature method (DQM) and non-dominated sorting genetic algorithm II (NSGA-II), by applying the system of the (FSDT) first-order shear deformation theory of plates and the differential quadrature method DQM the governing equations are obtained. Then, the DQM is connected with the optimal model of NSGA-II, and the trade-off is obtained with respect to fiber orientations between the objectives, and by applying the model of Young bargaining the best fiber orientations are obtained. **(A.V. Duran, et al., 2015)** presented thermal buckling analysis of square composite laminates with different stiffness properties. Based on the finite element and classical lamination theory the thermal buckling for many laminates is found, to resist thermal buckling are found the optimal fiber paths and under

constant thermal load for symmetrically balanced laminates is scrutinized thermal responses for multiple material models. The coefficients of thermal expansion are differentiated to research the influence on the optical fiber path and the critical temperature of buckling. This research obtains in comparison to straight fiber configurations, curved fiber path configurations increase of resistance to thermal buckling that provide a 36:9%. **(Jinqiang Li, et al., 2016)** studied the influence of random system properties of critical thermal buckling temperature of composite laminated plates through temperature-dependent properties by applying a micromechanical approach, depends on the CLPT in coupling by Hamilton's basic. To find the second-order statistics (mean and standard deviation) of the critical thermal buckling temperature they are applying a mean-centered first-order perturbation technique. Of random volume fractions, material properties, coefficients of thermal expansion, angels of layer, aspect ratios, and B. Cs, their effect on the critical temperature of thermal buckling is studied. **(M. Cetkovic, 2016)** by applying the Layerwise Theory of Reddy were subdued employing the (PVD) principle of virtual displacements the thermal of buckling laminated plates of the composite are studied. The isoparametric finite element approximation is found from the weak term, while the strong term is discretized utilizing the solution of Navier's analytical. The influencing on thermal buckling of isotropic, orthotropic, and laminated composite plates of ratio elastically E1/E2, side to thickness ratio, mesh refinement, ratio coefficient of thermal expansion, temperature distribution, aspect ratio, and B.Cs. **(S. Kamarian, et al., 2016)** applied a powerful meta-heuristic algorithm called a firefly algorithm (FA), which is based on the flashing behavior of fireflies to transact with stacking sequence optimization of laminated composite plates for maximizing the critical buckling temperature. The main objective of their study was to offer the capability of FA in the optimization of composite structures. **(Loc V. Tran, et al., 2017)** studied the two types of a thermal plate are take into consideration thermal bending and thermal buckling, a rise of temperature in structure plate produces normal non-zero transverse strain, a 6-variable model of quasi-3D, and one variable in displacement transverse of(HSDT) higher-order shear deformation theory to take into account. Thus, the effects of transverse shears and normal strain in a laminated composite plate are advanced. By (IGA) isogeometric analysis the governing equation is obtained. Because of the existence of bending coupling extension. **(Abdouna, et al., 2017)** a methodological approach based on the perturbation and homotopic methods is applied to study thermal buckling and post-buckling analyses with dependent properties on the temperature of the plates anisotropic laminated. A power law apportionment in the form of temperature is utilized, and to a uniform temperature difference, the structure is submitted. The method of finite element is applied for solutions numerically, the temperature and the displacement of power series expansions are progressing. The influence of structure geometry, boundary conditions and temperature-dependent properties on the thermal post-buckling and buckling behaviors are estimated. **(Rajesh Kumar, et al., 2017)** by distribution of uniform temperature by its thickness submitted to center on thermal heating on the plate area reported a solution of semi-analytical of thermal post-buckling and buckling of plate's rectangular composite. By fixing the thermos elasticity problem employs Airy's stress function the analytical terms for these in-plane allocation pre buckling stress during the composite plate are advanced. Applying a vibrational principle, the plate nonlinear stability equations are subedited, and applying First-order shear deformation theory incorporating von-Kármán geometric nonlinearity to model the plate. (Heated region area, aspect ratio, and the B.Cs) are examined the effect on the critical temperature of buckling and equilibrium paths.

This study investigates the critical temperature of buckling laminated composite thin plate with general boundary condition, based on classical laminated plate theory and using Rayleigh-Ritz method, the displacement function as Fourier cosine series plus a continuous function so the

effect of boundary conditions, aspect ratio, length to thickness ratio, angle-ply orientation, and different composite materials properties are examined.

2.THEORETICAL ANALYSIS
2.1 Classical Laminated Plate Theory
As a statically equivalent single layer owning complex constituent disposal are the equivalent single layer ESL laminated plate theories, so a variable properties laminated plate is processed, lessening the 3-D continuum problems to 2-D problems. By presuming the shape of the stress or displacement fields like a linear integration of unknown coordinate of thickness and functions, the equivalent single layer theories are amelioration: (**REDDY, 2004).**

$$\psi_i(x,y,z,t) = \sum_{j=0}^{N}(z)^j\psi_i^j(x,y,t) \tag{1}$$

Where ψ_i, z, (x,y), ψ_i^j,t, are the stress or displacement component, the coordinate of thickness, the plane coordinates, functions and time to be determined respectively. The governing equations ψ_i^j are calculated with the formulation of factual displacement, when ψ_i are displacements. The ESL is (CLPT)the classical plate laminated theory, which is a widening of the (classical) plate Kirchhoff theory to laminated plates of composite be based on the displacements field.

$$u(x,y,z,t) = u_o(x,y,t) - z\frac{\partial w_o}{\partial x}$$
$$v(x,y,z,t) = v_o(x,y,t) - z\frac{\partial w_o}{\partial y}$$
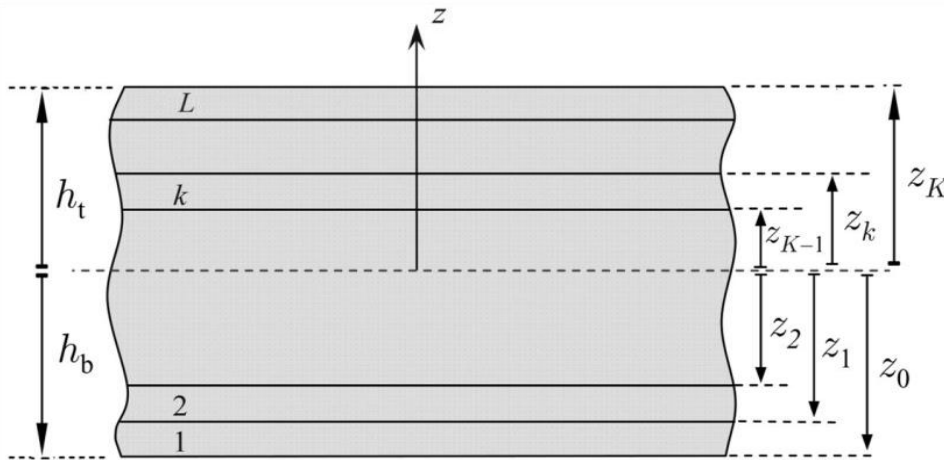$$w(x,y,z,t) = w_o(x,y,t) \tag{2}$$

Figure 1. Distances from the reference plane, (**Autar K. Kaw, 2006).**

Where the coordinate direction (x, y, z) the (u_o, v_o, w_o) are the displacement component, respectively, at the mid-plane (i.e., z = zero).
The differential equation of a thin laminated plate under thermal buckling load is written as: (**Henry Khov, 2009).**

$$D_{11}\frac{\partial^4 w}{\partial x^4} + (2D_{12} + 4D_{66})\frac{\partial^4 w}{\partial x^2\partial y^2} + D_{22}\frac{\partial^4 w}{\partial x^4} + 4D_{26}\frac{\partial^4 w}{\partial x\partial y^3} + 4D_{16}\frac{\partial^4 w}{\partial x^3\partial y} + N_X^T\frac{\partial^2 w}{\partial x^2} + N_y^T\frac{\partial^2 w}{\partial y^2} +$$
$$2N_{xy}^T\frac{\partial^2 w}{\partial x\partial y} = 0 \tag{3}$$
Where:

$$\{N^T\} = \sum_{k=1}^{L} \int_{h_{k-1}}^{h_k} [A]\{\alpha\}^k \, \Delta T \, dz \tag{4}$$

Where:

{α}   Vector of thermal expansion coefficient

[A]   Extension stiffness matrix

In this study, the uniform temperature distribution is taken into consideration. The plate temperature is initially supposed to be T_i where final temperature is uniformly raised to critical value T_{cr} in which the plate buckles. The temperature variation is then

$$\Delta T = T_{cr} - T_i \tag{5}$$

2.2 Boundary Conditions:

The twisting and bending, shear forces can express of the displacement function as (**Henry Khov, 2009**).

$$M_x = -D_{11} \frac{\partial^2 w}{\partial x^2} - D_{12} \frac{\partial^2 w}{\partial y^2} \tag{6}$$

$$M_y = -D_{22} \frac{\partial^2 w}{\partial y^2} - D_{12} \frac{\partial^2 w}{\partial x^2} \tag{7}$$

$$M_{xy} = -2D_{66} \frac{\partial^2 w}{\partial x \partial y} \tag{8}$$

$$Q_x = -D_{11} \frac{\partial^3 w}{\partial x^3} - (D_{12} + 4D_{66}) \frac{\partial^3 w}{\partial y^2 \partial x} \tag{9}$$

$$Q_y = -D_{22} \frac{\partial^3 w}{\partial y^3} - (D_{12} + 4D_{66}) \frac{\partial^3 w}{\partial x^2 \partial y} \tag{10}$$

For a pliably limited rectangular plate, the boundary conditions are

$$k_{x0}w = Q_x \qquad K_{x0} \frac{\partial w}{\partial x} = -M_x \qquad \text{at } x = 0 \qquad (11)(12)$$

$$k_{x1}w = -Q_x \qquad K_{x1} \frac{\partial w}{\partial x} = -M_x \qquad \text{at } x = a \qquad (13)(14)$$

$$k_{y0}w = Q_y \qquad K_{y0} \frac{\partial w}{\partial y} = -M_y \qquad \text{at } y = 0 \qquad (15)(16)$$

$$k_{y1}w = -Q_y \qquad K_{y1} \frac{\partial w}{\partial y} = -M_y \qquad \text{at } y = b \qquad (17)(18)$$
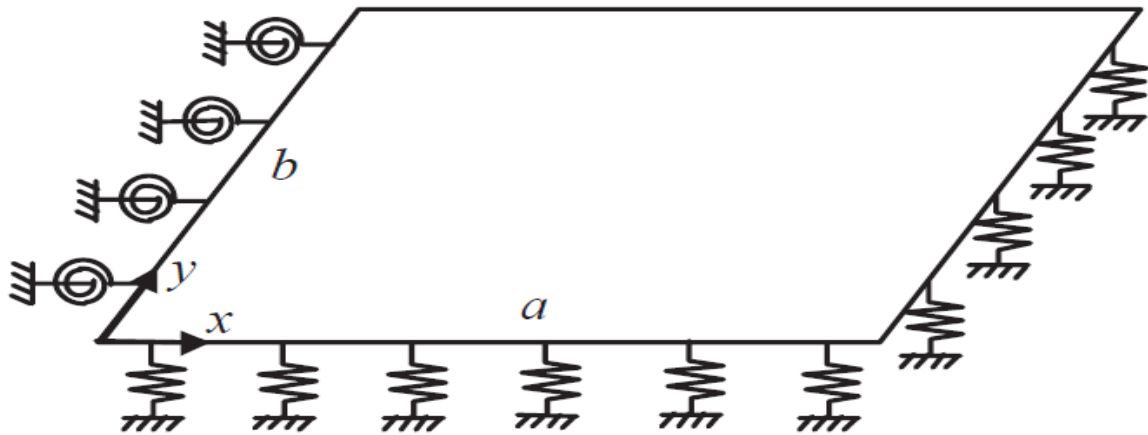

Figure 2. Elastically restrained of rectangular plate along edges, (**W. L. Li, 2004**).

Where K_{y0}, K_{y1} and K_{x0}, K_{x1} are the stiffness of spring in rotations, k_{y0}, k_{y1} and k_{x0}, k_{x1} are the stiffness of spring in transitional, $at\ y = 0\ and\ b(x = 0\ and\ a)$, respectively. Eq. (11) - (18) explain a set of different B.Cs from which, the free boundary condition can be found by putting the spring constant to zero while by setting the spring constant into infinity the clamped condition can be got (in actual calculation as a large number) and the simply supported can be obtained by setting the spring constant in between larger than 0 and small than ∞ ($0 < K < \infty$). **Fig. 2**.

Form Eq. (6)-(18), the boundary conditions can be finally expressed as:

$$k_{x0}w = -D_{11}\frac{\partial^3 w}{\partial x^3} - (D_{12} + 4D_{66})\frac{\partial^3 w}{\partial y^2 \partial x} \qquad (19)$$

$$k_{x1}w = D_{11}\frac{\partial^3 w}{\partial x^3} + (D_{12} + 4D_{66})\frac{\partial^3 w}{\partial y^2 \partial x} \qquad (20)$$

$$K_{x0}\frac{\partial w}{\partial x} = D_{11}\frac{\partial^2 w}{\partial x^2} + D_{12}\frac{\partial^2 w}{\partial y^2} \qquad (21)$$

$$K_{x1}\frac{\partial w}{\partial x} = D_{11}\frac{\partial^2 w}{\partial x^2} + D_{12}\frac{\partial^2 w}{\partial y^2} \qquad (22)$$

2.3 Admissible Functions:

The permissible functions take a significant rule in the Rayleigh-Ritz technique. The beam functions products are the orderly selection as the permissible functions, and the displacement function can be written as **(W.L. Li, 2004)**.

$$w(x, y) = \sum_{m,n=1} A_{mn} X_m(x) Y_n(y) \qquad (23)$$

Where $X_m(x)$ or $Y_n(y)$ are the characteristic beams functions containing the same B.Cs in the x-direction and y-direction, sequentially.

As a linear collection of trigonometric and hyperbolic functions, the functions of beam can be broadly acquired. They contain a few unbeknown parameters, and from the boundary conditions are obtained. Accordingly, then, all boundary conditions essentially drive to various forms of beam functions. In veritable employments, this is plainly inappropriate, for a various boundary beam not to remember the boredom of obtaining the characteristic functions. An advanced method of Fourier series has been suggested for beams with qualitative boundary at ends to eschew this obstacle, in which the characteristic functions are express in the term of **(Li, 2000).**

$$w(x) = \sum_{m=0}^{\infty} a_m \cos \lambda_{am} x + p(x)\left(\lambda_{am} = \frac{m\pi}{a}\right),\ 0 \le x \le a. \qquad (24)$$

Where p (x) can be a counted a qualitative continuous function that, whatever of B.Cs, is permanently elected to accept the subsequent equations:

$P'''(0) = W'''(0) = \alpha_0,$ $P'''(a) = W'''(a) = \alpha_1,$ (25)(26)

$P'(0) = W'(0) = \beta_0,$ $P'(a) = W'(a) = \beta_1,$ (27)(28)

Still, as a continuous function that accepts **Eq. (25)-(28)**, p(x) has only been understood, its formula isn't worried by consideration to the convergence of the series of the solution. Thus, the function p (x) can be option in different wanted shapes. As shown, postulate that p (x) is a polynomial function

$$P(x) = \sum_{n=0}^{4} C_n P_n \left(\frac{x}{a}\right) \tag{29}$$

Where $P_n(x)$ is the Legendre function C_n is the expansion constant of order n.
The above expression for the function P(x) can be expressed as:

$$P(x) = \zeta_a(x)^T \bar{\alpha} \tag{30}$$

Where

$$\bar{\alpha} = \{\alpha_0, \alpha_1, \beta_0, \beta_1\}^T \tag{31}$$

And

$$\zeta_a(x)^T = \begin{Bmatrix} -(15x^4 - 60ax^3 + 60a^2x^2 - 8a^4)/360a \\ (15x^4 - 30a^2x^2 + 7a^4)/360a \\ (6ax - 2a^2 - 3x^2)/6a \\ (3x^2 - a^2)/6a \end{Bmatrix} \tag{32}$$

The results in Eq. (30)-(32) are obtained from much directly, but little general approaches (**Li, 2004**).

To find the unknown the coefficient of boundary, $\alpha_0, \alpha_1, \beta_0$, and β_1, substitution of **Eq. (24)** and **(30)** into the boundary conditions **Eq. (19)-(22)** results in:

$$\bar{\alpha} = \sum_{m=0}^{\infty} H_a^{-1} Q_{am} a_m \tag{33}$$

Where

$$H_a = \begin{bmatrix} 1 + \dfrac{8k_{x0}a^3}{360D_{11}} & \dfrac{7k_{x0}a^3}{360D_{11}} & \dfrac{-k_{x0}a}{3D_{11}} & \dfrac{-k_{x0}a}{6} \\ \dfrac{7k_{x1}a^3}{360D_{11}} & 1 + \dfrac{8k_{x1}a^3}{360D_{11}} & \dfrac{-k_{x1}a}{3D_{11}} & \dfrac{-k_{x1}a}{6} \\ \dfrac{a}{3} & \dfrac{a}{6} & \dfrac{K_{x0}}{D_{11}} + \dfrac{1}{a} & \dfrac{-1}{a} \\ \dfrac{a}{6} & \dfrac{a}{3} & \dfrac{-1}{a} & \dfrac{K_{x1}}{D_{11}} + \dfrac{1}{a} \end{bmatrix} \tag{34}$$

$$Q_{am} = \left\{(-1)\dfrac{k_{x0}}{D_{11}} (-1)^m \dfrac{k_{x1}}{D_{11}} \quad -\lambda_{am}^2 (-1)^m \lambda_{am}^2 \right\}^T \tag{35}$$

For a totally free beam, the matrix Ha will be one matrix. Via, this case can be controlled to a few stretches by fictitious deliver springs to the edges of a beam with littlest stiffness. It has been exhibited in (**Li, 2002**). In such remediation via the matrix might be unconditional, although the functions are much appropriate for specific conditions and can be instantly applied in the method of Rayleigh-Ritz as the permissible functions.

By applying **Eq. (30)** and **(33)**, **Eq. (24)** expressed as

$$w(x) = \sum_{m=0}^{\infty} a_m \varphi_m^a(x) \tag{36}$$

Where

$$\varphi_m^a(x) = \cos \lambda_{am} x + \zeta_a(x) H_a^{-1} Q_{am} \tag{37}$$

Mathematically, **Eq. (36)** suggest that all of the functions of the beam shown as a function in the practical area with the principal functions $\{\varphi_m^a(x): m = 0, 1, 2, \dots\}$. Therefore, **Eq. (23)** expressed as:

$$w(x,y) = \sum_{m,n=0}^{\infty} A_{mn} \varphi_m^a(x) \varphi_n^b(y) \tag{38}$$

Where

$$\varphi_n^b(y) = \cos \lambda_{bn} y + \zeta_b(y) H_b^{-1} Q_{bn} \tag{39}$$

The terms for $\zeta_b(y), H_b$ and Q_{bn} can be, correspondingly, found from **Eq. (32), (34)** and **(35)** by little shifting the x- concerning parameters by the y- concerning.

2.4 Determination of Critical Buckling Temperature:

The plate is applied to thermal buckling load N_x^T, N_y^T and N_{xy}^T respectively. The total mechanical energy can be formed in the following terms:

$$
\begin{aligned}
E = \frac{1}{2} \int_0^b \int_0^a & \left[D_{11} \left(\frac{\partial^2 w}{\partial x^2} \right)^2 + D_{22} \left(\frac{\partial^2 w}{\partial y^2} \right)^2 + D_{66} \left(\frac{2\partial^2 w}{\partial x \partial y} \right)^2 + 2 \left(D_{12} \frac{\partial^2 w}{\partial x^2} \frac{\partial^2 w}{\partial y^2} \right) \right] dx\, dy \\
& + \frac{1}{2} \int_0^b \left[k_{x0} w^2 + K_{x0} \left(\frac{\partial w}{\partial x} \right)^2 \right]_{x=0} dy + \frac{1}{2} \int_0^b \left[k_{x1} w^2 + K_{x1} \left(\frac{\partial w}{\partial y} \right)^2 \right]_{x=a} dy \\
& + \frac{1}{2} \int_0^a \left[k_{y0} w^2 + K_{y0} \left(\frac{\partial w}{\partial y} \right)^2 \right]_{y=0} dx + \frac{1}{2} \int_0^a \left[k_{y1} w^2 + K_{y1} \left(\frac{\partial w}{\partial y} \right)^2 \right]_{y=b} dx \\
& - \frac{1}{2} \int_0^b \int_0^a \left[N_x^T \left(\frac{\partial w}{\partial x} \right)^2 + N_y^T \left(\frac{\partial w}{\partial y} \right)^2 + 2 N_{xy}^T \left(\frac{\partial^2 w}{\partial x \partial y} \right) \right] dx\, dy \tag{40}
\end{aligned}
$$

Where the transverse deflection (w_o) is replaced as aforementioned in section (2.3) to obtain the critical buckling Temperature substituting **Eq. (5)** in **(4)** and then in **Eq. (40)**. Proceeding the wanted of differentiations and integrations of **Eq. (40)** after that putting the mechanical energy in form of:

$$\frac{\partial E}{\partial A_{mn}} = 0 \tag{41}$$

Eq. (41) allows homogenous equations as follow:

$$f(A_{mn}, \Delta T_{cr}) = 0 \text{ For thermal buckling temperature problem} \tag{42}$$

Eq. (42) fixing as an Eigen-value problem which is express as below:

$$
\begin{bmatrix} a_{1,1} & \cdots & a_{1,(m*n)} \\ \vdots & \ddots & \vdots \\ a_{(m*n),1} & \cdots & a_{(m*n),(m*n)} \end{bmatrix} \begin{Bmatrix} A_{11} \\ \vdots \\ A_{mn} \end{Bmatrix} = 0 \tag{43}
$$

Where a_{ij} are the coefficient of the nonzero impersonality A_{mn}. Obtained the first term determinant of **Eq. (43),** and equating it to zero to find critical buckling temperature. The ΔT_{cr} is obtained by fixing the eigenvalue problem. For M and N more than 1and various edge conditions, the analysis's solution will be complicated, so it must use computer programming to

find ΔT_{cr}. In this investigation, MATLAB R2017b is applied to fix the eigenvalue problem to obtain the critical buckling temperature.

1. Numerical Results

With elastic boundary conditions supported the laminated plate is assumed to be embedded in thermal environments by a uniform temperature rise in the depth of the plate, by eigenvalue problem results from Ritz solution, its critical temperature of the buckling is determined. To verify the buckling temperature of thin plates calculated based on the admissible function used and activity of the computer program using Matlab 17 presented results are compared with those obtained by other researchers. Antisymmetric angle laminated plates are in good agreement when compared with those obtained by (**Houdayfa, et al., 2014**) and (**Sarath, 2000**). Although they used different solution methods as shown in **Table 1,** the plate contains 10 layers with various orientations angles and simply supported in all edges are possessed to investigate the influence of the fiber angle on the critical temperature of buckling, higher lamina angle leads to higher critical temperature of an antisymmetric angle plies for angles $(0^o - 45^o)$. This is due to the increase of stiffness and thus increase the critical temperature of buckling. For numerical results, the material properties are $E_1 = 15\text{Gpa}$, $E_2 = 1\text{Gpa}$, $G_{12} = 0.5\text{Gpa}$, $v_{12} = 0.3$, $\alpha_1 = 0.015*10^{-6}$ $1/^o C$, $\alpha_2 = 1*10^{-6}$ $1/^o C$,

Table 1. The critical temperature of buckling at angle-ply simply supported square composite plates, $\Delta Tcr = Tcr * \alpha_2$, N=10, thickness ratio =100.

θ	Present	C. Sarath Babu T. Kant	Discrepancy %	OUNIS et al	Discrepancy %
0	$0.75246 * 10^{-3}$	$0.7463* 10^{-3}$	0.81865	$0.7846 * 10^{-3}$	4.1
15	$0.114 * 10^{-2}$	$0.1115* 10^{-2}$	2.193	$0.1133 * 10^{-2}$	0.614
30	$0.15467 * 10^{-2}$	$0.1502* 10^{-2}$	2.89	$0.154 * 10^{-2}$	0.4332
45	$0.17277 * 10^{-2}$	$0.1674* 10^{-2}$	3.108	$0.172 * 10^{-2}$	0.44568

Two types, symmetric cross and angle ply-simply supported plates (eight layered) under uniform temperature are investigated in **Table 2,** compared by the results obtained by (**Houdayfa, et al., 2014**) using a finite element based upon the classical plate theory. It is well seen that critical temperature of angle ply greater than cross-ply due to the increase of the stiffness and thus increase the critical temperature of buckling, it is shown that numerical results are in good agreement, the material properties are $E_1 = 22.5\text{Mpa}$, $E_2 = 1.17\text{Mpa}$, $G_{12} = 0.66\text{Mpa}$, $v_{12} = 0.22$, $\alpha_1 = -0.04*10^{-6}$ $1/^o C$, $\alpha_2 = 16.7*10^{-6}$ $1/^o C$

Table 2. Critical buckling temperature of simply supported composite laminated plates, ΔTcr $(^o C)$, a=15, b=12, h=0.048

θ	Present	OUNIS et al	Discrepancy %
(0/90/90/0)ₛ	12.29708	12.2716	0.2072
(0/45/-45/90)ₛ	14.17358	13.7388	3.06754

In **Table 3** the critical buckling temperature of laminated plate with different thickness ratio are compared with published results of (**Achchhe, et al., 2009).** The example of plate have stacking sequence of [45/-45]$_{3T}$ with simply supported in all edges applied to uniform temperature distributions, as noted the decrease in thickness ratio increases the buckling temperature due to stiffness increase of plate so it needs high temperature to buckle, the results of present study are very close to those obtained by Achchhe Lal et al. using HSDT, the material properties are E_1=0.081Gpa, E_2=10.3Gpa, G_{12}=0.031Gpa, G_{23}=0.0304Gpa v_{12}=0.21, $α_1$= -0.21*10^{-6} 1/°C, $α_2$=16*10^{-6} 1/°C, $α_0$ = 1*10^{-6} 1/°C.

Table 3. Comparison of buckling loads $ΔTcr$ (°C) for perfect, angle-ply $(±45)_{3T}$ square laminated composite plates having simply supported boundary conditions $ΔTcr=Tcr*α_0*10^3$

a/h	Present	Achchhe Lal et al	Discrepancy %
100	0.13175	0.1283	2.6186
80	0.206	0.1998	3.01
50	0.527	0.4873	7.5332
40	0.82342	0.7806	5.2
30	1.464	1.3591	7.1653

The critical temperature of four-layered cross-ply symmetric laminated thin plates with various boundary conditions are compared in **Table 4** with results obtained by (**Rajesh Kumar, et al., 2017).** They used, first-order shear deformation theory to model the plate and also compared by (**Kamariana, et al., 2016)** who showed that the temperature buckling is highest in CCCC boundary condition and lowest in SSSS boundary condition because the stiffness of clamped is the larger than simply supported plate. Also the numerical results show good agreement, where the material properties are E_1=15Gpa, E_2=1Gpa, G_{12}=0.5Gpa, G_{23}=0.3356Gpa, v_{12}=0.3, $α_1$=0.015*10^{-6} 1/°C, $α_2$=1*10^{-6} 1/°C, $α_0$ = 1*10^{-6} 1/°C.

Table 4. Critical Buckling Temperature $ΔTcr = Tcr * α_0 *10^2$, a/b=1, a/h=100, (0/90/90/0)

B.C	Present	S. Kamariana et al	Discrepancy %	Rajesh Kumar et al	Discrepancy %
SSSS	0.1	0.0996	0.4	0.0999	0.1
CCCC	0.3653	0.3354	8.18	0.338	7.47
SCSC	0.1491	-----------	-----------	0.1467	1.61
CSCS	0.2593	-----------	-----------	0.2554	1.5

In **Table 5** another comparison is shown, with the closed-form solution based on the FSDT obtained by (**Mohammad-Zaman Kabir, et al., 2016);** plates with CCCC and SSSS boundary conditions with good agreement. Two materials are compared in this case, material 1 (E_1=38.16Gpa, E_2=9.65Gpa, G_{12}=6.21Gpa, v_{12}=0.26, $α_1$=4*10^{-6} 1/°C, $α_2$=16*10^{-6} 1/°C) and

material 2(E_1=155Gpa, E_2=8.07Gpa, G_{12}=4.55Gpa, v_{12}=0.22, α_1= -0.07*10^{-6}1/^{o}C, α_2=16*10^{-6}1/^{o}C).

Table 5. Critical Buckling Temperature ΔTcr (^{o}C) a=b=200mm, h=2mm, (0/90/0/90)

B.C	Present		Mohammad-Zaman Kabir et al		Discrepancy %	
Materials	1	2	1	2	1	2
SSSS	17.8	53.4122	18	53.1	1.1236	0.58451
CCCC	55.376	208.0555	54.8	195.4	1.04	6.082526
SSCC	31	104.244	33.8	105.1	9.0322	0.82115

Effect of aspect ratio on critical temperature of laminated angle plate is obtained in **Table 6;** results are compared with (**Wen-Chi Chen, et al., 1993),** who used first-order transverse shear deformation theory. It is noted that increasing the aspect ratio increases the buckling temperature due to the increase in the stiffness of the plate. The accuracy of the present approach is validated for evaluating the influence of aspect ratio on the critical buckling temperature; the material properties are E_1=40Gpa, E_2=1Gpa, G_{12}=0.5Gpa, G_{23}=1Gpa v_{12}=0.25, α_1=1*10^{-6} 1/^{o}C, α_2=1*10^{-6} 1/^{o}C.

Table 6. Critical Buckling Temperature ΔTcr (^{o}C), a /h=100, (45/-45)

a/b	Present	Wen-Chi Chen et al	Discrepancy %
0.125	46.1762	45.356	1.77624
0.375	68.031	66.579	2.134
0.625	102.863	100.528	2.27
0.875	142.344	138.950	2.38
1	162.5832	158.608	2.445
1.125	182.9885	178.391	2.5123

Table 7 shows the influence of rotational stiffness spring on the critical buckling temperature the value of rotational stiffness spring coefficient in simply support is Zero while for clamped edges coefficient of rotational spring is large number; critical temperature increases when the rotational stiffness spring coefficient is increased as mentioned before, the material properties E_1=40Gpa, E_2=1Gpa, G_{12}=0.5Gpa, v_{12}=0.25, α_1=1*10^{-6} 1/^{o}C, α_2=2*10^{-6} 1/^{o}C.

Table 7. Critical Buckling Temperature ΔTcr (^{o}C), a /h=100, a/b=1, 0/90/90/0)

K	0	1e1	1e2	1e3	1e4	1e5	1e6	1e7	1e8	1e9	1e10
result	83.78 (SSSS)	83.97	85.64	100.5	264.7	270	288.73	290.9	291.13	291.15	291.15 (CCCC)

The influence of other boundary conditions on critical buckling temperature for the plate with a symmetric and antisymmetric cross and angle ply is shown in **Table 8**. Some of the results are compared with (**Wen-Chi Chen, et al., 1993).** The publisher used first-order transverse shear deformation theory for antisymmetric angle ply, properties of material are E_1=25Gpa, E_2=1Gpa, G_{12}=0.5Gpa,G_{23}=0.2Gpa, v_{12}=0.25, α_1=1*10^{-6} 1/^{o}C, α_2=3*10^{-6} 1/^{o}C.

Table 8. Critical Buckling Temperature $\Delta Tcr = Tcr *((a/h)^2)* \alpha_1*10$, a /h=50, a/b=1

B.C	SSSF	SFSF	SCSF
Stacking sequence	Present		
(45/-45)$_2$	6.364	4.007	7.108
Wen-Chi Chen et al	7.177	3.607	8.510
Discrepancy %	12.76	9.98	19.7
(45/-45)$_s$	6.39	4.0351	7.123
(0/90)$_2$	5.693	3.952	5.7348
(0/90)$_s$	2	1.644	2.9457

The effect of different (ratio of modulus elastically (E1/E2) and the ratio of thermal expansion coefficient ($\alpha2/\alpha1$) on critical temperature of a symmetric and antisymmetric angle-ply and cross-ply 4-layer simply supported and clamped edges plate applied to uniform temperature distribution is tested. Material properties are: E_2=1Gpa, G_{12}=0.5Gpa, v_{12}=0.25, α_1=1*10^{-6} 1/^{o} C, α_2=2*10^{-6} 1/^{o}C, a/h=100, a/b =1. In **Fig. 3** and **4** for cross-ply and angle symmetric and antisymmetric plate the simply and clamped supported plate, there is small change (inversely) in stiffness of laminates with increase in E_1. It should be observed that coupling between extensions and bending is not taken in this investigation. The influence of coupling is clearer in anti-symmetric angle -ply laminates. From **Fig. 5** and **6,** it is obvious that the critical temperature of buckling lowering as the thermal expansion ratio raises, exhibit the effect of thermal expansion coefficient ratio ($\alpha2/\alpha1$) on critical temperatures of plates when E_1=40Gpa, as shown in **Fig. 5** and **6** for cross and angle ply plate the simply and clamped supported plate for symmetric and antisymmetric, there is an inverse proportionality between the critical buckling temperature parameter and ($\alpha2/\alpha1$) due to the stiffness of plate decreasing as the thermal expansion coefficient ratio ($\alpha2/\alpha1$) increase. In this study, analysis E_1=40Gpa and α_2 are diverse when α_1 is staying constant.
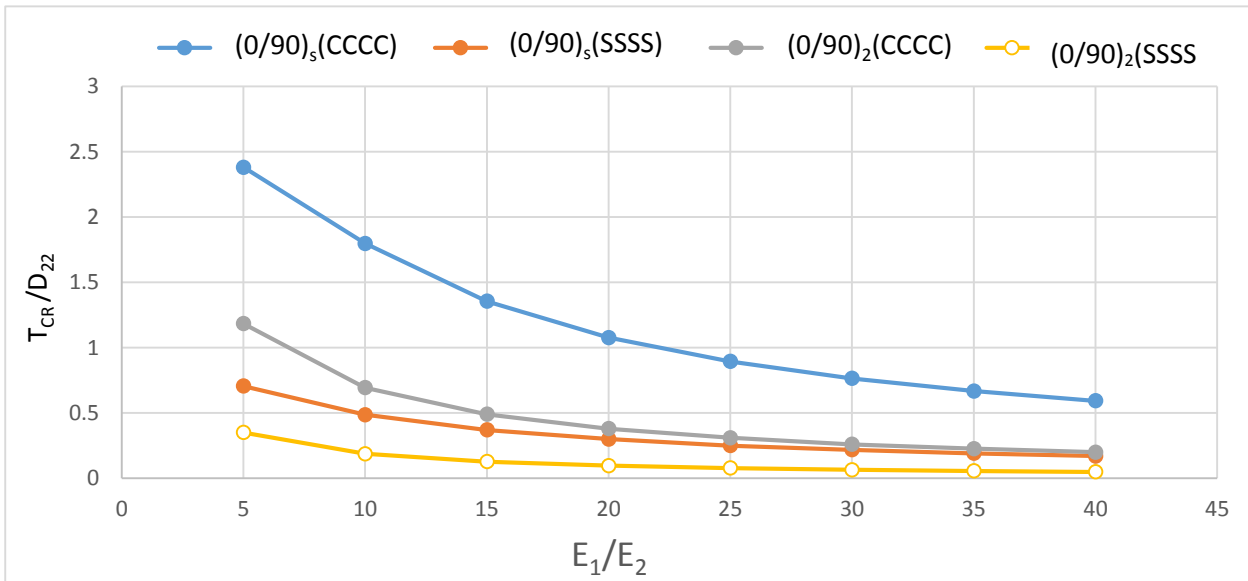
Figure 3. Change of the ratio elastically (E_1/E_2) on critical temperature Tcr/D_{22} at the cross plate.
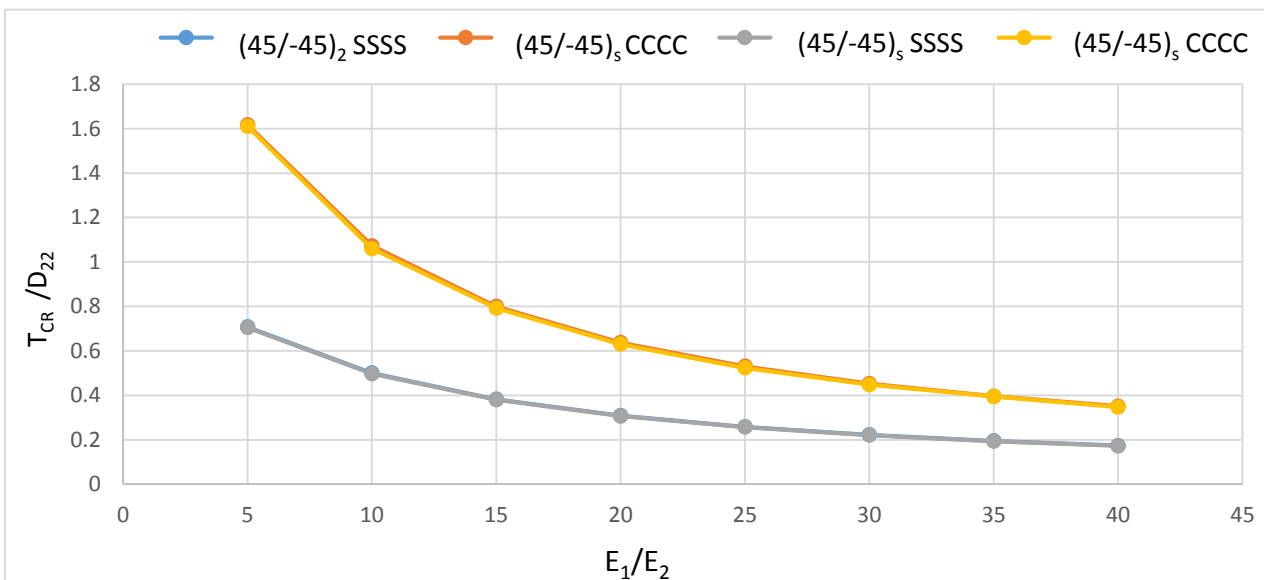

Figure 4. Change of the ratio elastically (E_1/E_2) on critical temperature Tcr/D_{22} at angle plate.
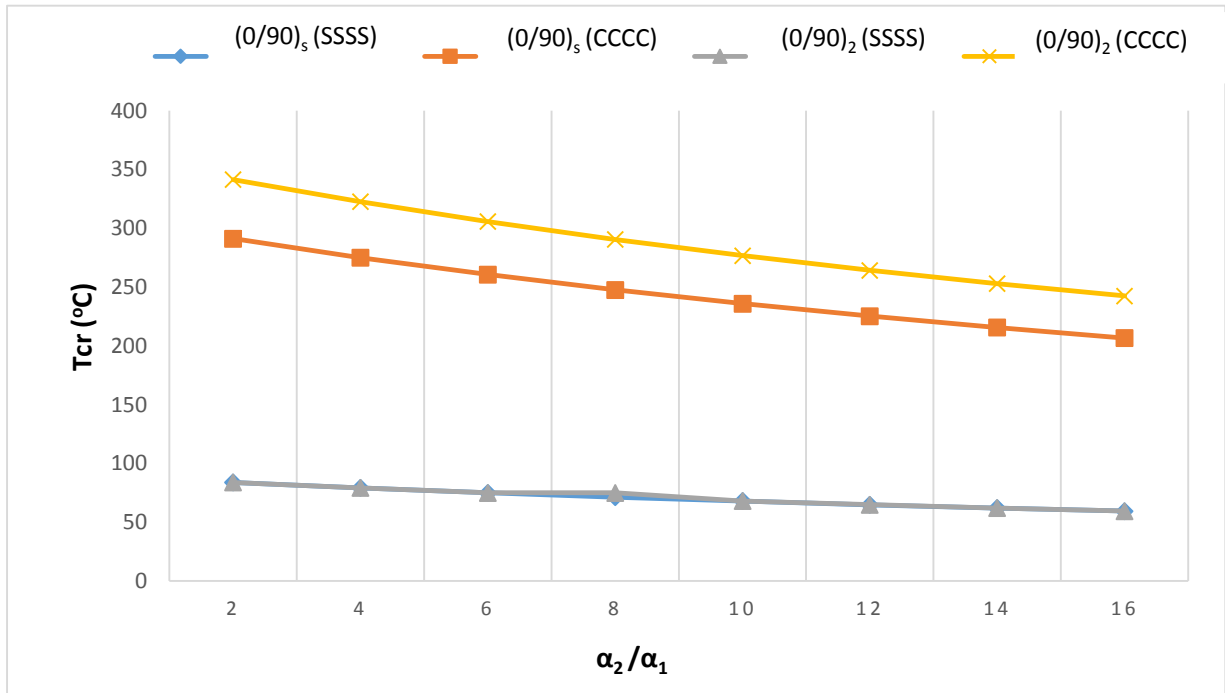
Figure 5. Change of the ratio coefficient (α_2/α_1) on critical temperature Tcr (^{o}C) at cross-ply.
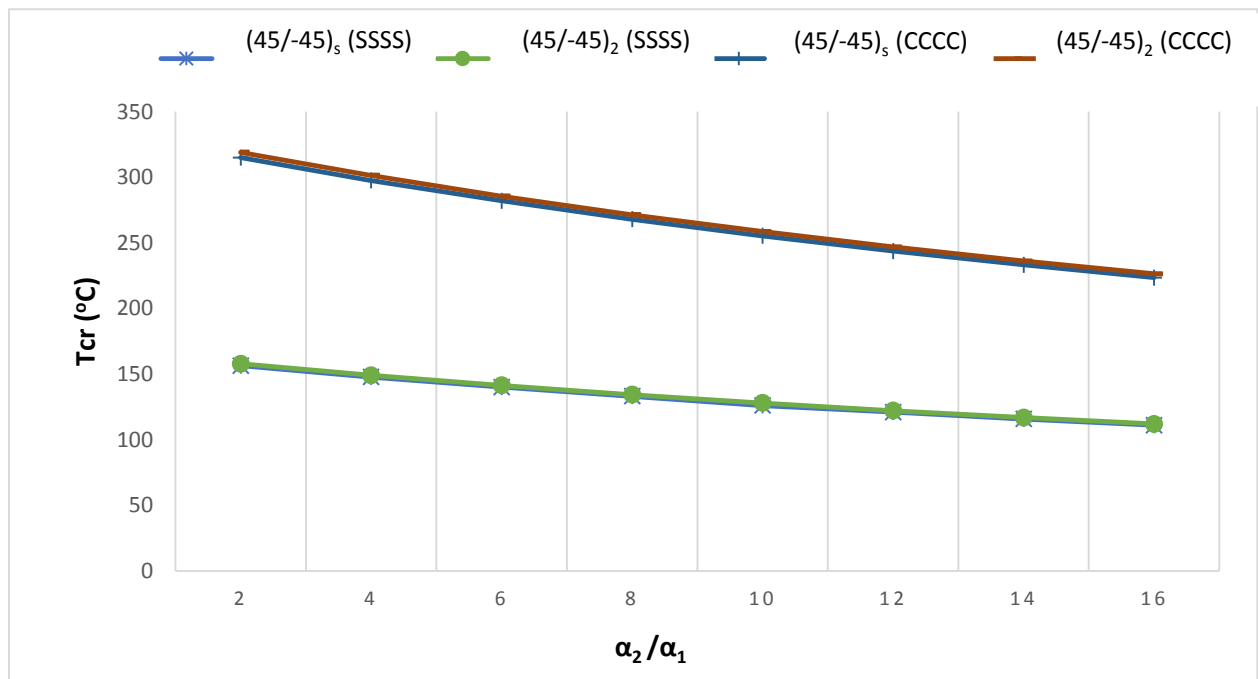

Figure 6. Change of the ratio coefficient (α_2/α_1) on critical temperature Tcr (^{o}C) at angle ply.

CONCLUSIONS

In the present work, the critical buckling temperature of a composite laminated cross and angle plates with general boundary conditions is developed using the Ritz method based on a function proposed by **(Li, 2002)** for the first time.

The obtained results are compared with those found by many researchers who studied thermal buckling of a composite laminated by different solution methods. The main conclusions from obtained results as excepted, are:

1- The influence of boundary conditions on the critical temperature buckling is very clear. Clamped edges conditions result in high critical temperature buckling due to offering high stiffness compared by the simply and free, supported conditions.

2- The critical temperature buckling is inversely proportional to design parameters (aspect ratio, thickness ratio, lamination angle, modulus elastically ratio (E1/E2) and thermal expansion ratio (α1/α2)).

3- The angle ply gives higher critical temperature buckling than cross-ply for the same materials.

REFERENCES:

- A.R.Vosoughi and M.R.Nikoo, 2015. Maximum fundamental frequency and thermal buckling temperature of laminated composite plates by a new hybrid multi-objective optimization technique. Journal of Thin-Walled Structures, 95 (2015)408–415.

- A.V. Duran, et al., 2015. Thermal buckling of composite plates with spatial varying fiber orientations. Journal of Composite Structures, S0263-8223(14)00731-4.

- Achchhe Lal, et al., 2009. Effects of random system properties on the thermal buckling analysis of laminated composite plates. Journal of Computers and Structures, 87 (2009) 1119–1128.

- Autar K. Kaw, 2006. Mechanics of Composite Materials, 2nd ed., CRC Press, Taylor and Francis Group, 2006.

- C. Sarath Babu T. Kant, 2000. Refined higher order finite element models for thermal buckling of laminated composite and sandwich plates. Journal of Thermal Stresses, 23:111-130, 2000.

- Eduard Ventsel and Theodor Krauthammer, 2001. Thin Plates and Shells (Theory, Analysis, and Applications). The Pennsylvania State University, University Park, Pennsylvania.

- F. Abdouna, et al., 2017, Thermal buckling and post-buckling of laminated composite plates with temperature dependent properties by an asymptotic numerical method. Corresponding author: LAMAT, Higher School of Technical Education of Rabat (ENSET), Mohammed V, University in Rabat, Rabat, Morocco, and E-mail address: farahaboun@yahoo.fr.

- Hasanain Ibraheem Nsaif, et al., 2012. Buckling Analysis of Composite Plates under Thermal and Mechanical Loading. Journal of Engineering, Number 12 Volume 18 December 2012.

- Henry Khov, et al., 2009. An accurate solution method for the static and dynamic deflections of orthotropic plates with general boundary conditions. Composite Structures, 90, 474–481.

- Hiroyuki Matsunaga, 2006. Thermal buckling of angle-ply laminated composite and sandwich plates according to a global higher-order deformation theory, Journal of Composite Structures, 72 (2006) 177–192.
- Houdayfa OUNIS, et al., 2014. Thermal buckling behavior of laminated composite plates: a finite-element study. Journal of Front. Mech. Eng. 2014, 9(1): 41–49.
- J.N. REDDY, 2004. Mechanics of Laminated Composite Plates and Shells: Theory and Analysis, 2nd ed., CRC Press LLC.
- Jean-Marie Berthelot, 2010. Mechanics of Composite Materials and Structures, 3rd ed. ISMANS, Institute for Advanced Le Mans, Materials and Mechanics, France.
- Jinqiang Li, et al., 2016. Stochastic thermal buckling analysis of laminated plates using perturbation technique. Journal of Composite Structures, 139 (2016) 1–12.
- L. Aszlo P. Kollar and George S. Springer, 2003. Mechanics of Composite Structures, Cambridge University Press.
- Le-Chung Shiau, et al., 2010. Thermal buckling behavior of composite laminated plates. Composite Structures. 92 (2010) 508–514.
- Loc V. Tran, et al., 2017. Isogeometric finite element approach for thermal bending and buckling analyses of laminated composite plate. Journal of Composite Structures, S0263-8223(17)30714-6.
- M. Cetkovic, 2016. Thermal buckling of laminated composite plates using layerwise displacement model. Journal of Composite Structures, 142 (2016) 238–253.
- Mohammad-Zaman Kabir and Behrang Tavousi Tehrani, 2016. Closed-form Solution for Thermal, Mechanical, and Thermo-Mechanical Buckling and Post-buckling of SMA Composite Plates. Journal of Composite Structures, S0263-8223(16)31795-0.
- Rafat Assad Ghani, et al., 2017. Free Vibration Analysis of Laminated Composite plates with General Elastic Boundary Supports. Journal of Engineering, Number 4 Volume 23 April 2017.
- Rajesh Kumar, et al., 2017. Semi-analytical approach for thermal buckling and post buckling response of rectangular composite plates subjected to localized thermal heating. Journal of Acta Mech, DOI 10.1007/s00707-016-1797-9.
- S. Kamarian, et al., 2016. Thermal buckling optimization of composite plates using firefly algorithm. Journal of Experimental & Theoretical Artificial Intelligence, 1362-3079.
- Sandeep Singh, et al., 2013. Buckling of laminated composite plates subjected to mechanical and thermal loads using meshless collocations. Journal of Mechanical Science and Technology, 27 (2) (2013) 327~336.
- W.L. Li, 2000. Free vibrations of beams with general boundary conditions. Journal of Sound and Vibration. 237, 709–725.
- W.L. Li, 2004. Vibration analysis of rectangular plates with general elastic boundary supports. Journal of Sound and Vibration, 273, 619–635.
- Wen-Chi Chen and W. H. Liu, 1993. Thermal buckling of antisymmtric angle-ply laminated plates an analytical levy-type solution. Journal of Thermal Stresses, 16:401-419.

List of Symbols

Symbols	Description	Units
a, b	plate length and width, respectively	m
E	total mechanical and kinetic energies of a system	N.m

h	the thickness of the laminate	mm
h_t, h_b	thickness at the top and bottom of the laminate	mm
h_k, h_{k-1}	distances from the reference plane of the laminate to the two surfaces of the kth ply	mm
i, j	components of series	-----
$\kappa_x, \kappa_y, \kappa_{xy}$	curvatures of the reference plane of the plate	-----
k	layer number	-----
L	total number of layers in the laminate	-----
K_{x0}, K_{x1}	rotational stiffness at x = 0 and a, respectively	N.m/rad
K_{y0}, K_{y1}	rotational stiffness at y = 0 and b, respectively	N.m/rad
k_{x0}, k_{x1}	translational stiffness at x = 0 and a, respectively	N/m
k_{y0}, k_{y1}	translational stiffness at y = 0 and b, respectively	N/m
M, N	upper limits of double series	-----
NT	the resultant of thermal force	Pa.m
a_m	expansion or Rayleigh-Ritz coefficient	-----
U	the strain energy of deformation	N.m
u, v, w	displacements in x, y, z directions, respectively	m
u_o, v_o, w_o	displacements of the reference surface in the x, y, z directions, respectively	m
$W(X)$	flexural displacement of a beam	m
$w(x, y)$	flexural displacement of a plate	m
$w(x, y, t)$	dynamic displacement	m
P(x)	a simple polynomial function	-----
$X_m(x)$, $Y_n(y)$	beam characteristic function	-----
[A]	extension stiffness matrix	N/m
$\{\alpha\}$	vector of thermal expansion coefficient	$1/^{0}C$